

The hot compaction of polypropylene fibres

M. I. ABO EL-MAATY*, D. C. BASSETT‡, R. H. OLLEY

J.J. Thomson Physical Laboratory, Whiteknights, University of Reading, Reading RG6 6AF, UK

P. J. HINE, I. M. WARD

IRC in Polymer Science and Technology, University of Leeds, Leeds LS2 9JT, UK

Investigation of the compaction of unidirectionally arranged high-tenacity polypropylene fibres is described. A combination of techniques, with the major emphasis being morphological studies, show that controllable "selective" surface melting is not achieved at a high enough proportion to give substantial fibre-to-fibre bonding, and hence good lateral strengths.

1. Introduction

In a number of recent papers [1–5] we have described how the process of hot compaction can be used with high-modulus thermoplastic fibres, to manufacture samples of large section which retain a significant proportion of the original fibre modulus, by retaining a substantial percentage of the original fibre. The process works by selectively melting a small portion of the surface of each fibre, which on compaction and cooling recrystallizes to fill the interfibrillar voids. The papers published so far detail how effectively the process works with melt-spun polyethylene fibre [1] and polyethylene terephthalate fibre [2]. Structural analysis of the compacted materials, particularly for the melt-spun polyethylene fibre [3–5], show that the material is a composite of a fibrous phase embedded in a matrix of recrystallized lamellae. The lamellae grow out from the original fibre backbones in row structures, and form such a strong fibre-to-fibre bond that subsequent failure of the compacted material occurs within, rather than between, the fibres.

In this paper we describe experiments to investigate the compaction of high-tenacity unidirectionally arranged polypropylene fibres. A major portion of the paper is concerned with microstructural analysis investigating the morphology of the composites.

2. Experimental procedure

The work employed a unidirectional arrangement of fibres, and used a high-tenacity polypropylene (PP) fibre, trade name LEOLENE, manufactured by F. Drake and Company of Golcar Ltd, Huddersfield. The fibre had a linear density of 1008 denier, and its tensile modulus, measured on an Instron tensile testing machine at a strain rate of 10^{-4} s^{-1} , was 7.1 GPa.

2.1. Sample preparation

Samples of compacted polypropylene were produced under broadly similar conditions to those developed from the previous work on polyethylene (PE) and polyethylene terephthalate (PET) [1, 2]. The PP fibres were first wound on to a C-shaped former and then placed into a matched metal mould, dimensions 55 mm square. The assembly of fibres and mould was placed into a hot press set at the required compaction temperature and a holding pressure was applied while the assembly reached the compaction temperature. The role of the holding pressure was to restrain the fibres from shrinking and losing their orientation, while at the same time allowing controlled melting to occur. It can be appreciated that these two requirements often conflict and a balance has to be achieved. This balance is particularly difficult for PP fibres, where the shrinkage force can often be very high at temperatures close to the melting point. For these experiments a holding pressure of 1.1 MPa (150 p.s.i.) was employed, which compares with 0.7 MPa (100 p.s.i.) recommended for melt-spun polyethylene fibres and 1.9 MPa (270 p.s.i.) for polyethylene terephthalate fibres reported previously [1, 2]. Once the assembly reached the compaction temperature, it was left for a further 20 min to allow even heating. Finally, a compaction pressure of 14 MPa (2000 p.s.i.) was applied for 10 s before cooling the sample to 100 °C and removing from the hot press.

Samples were made at temperatures between 164 and 174 °C. Above 174 °C the fibres became too soft and extruded from the mould during the final higher pressure compaction.

2.2. Differential scanning calorimetry (DSC)

DSC analysis, widely used in the previous studies to assess the melting behaviour of the original fibres and

* Present address: Department of Physical Science, Faculty of Engineering, University of Mansoura, Mansoura, Egypt.

‡ Author to whom all communication should be addressed.

to measure the proportions of the original fibre and the melted and recrystallized phase, was also used in this current work, although on a much smaller scale. The lower crystallinity of the high-tenacity polypropylene fibre used in these studies, compared to the melt-spun PE fibres and PET fibres used previously, made this technique of less use here because it relies on measuring the crystalline melting behaviour. The result was that the morphological analysis, used in conjunction with DSC previously, had a much greater importance in this study as the only available technique for discerning the compaction mechanisms.

2.3. Electron microscopy

In the current study, compacted samples were cut open with glass knives on a microtome; sections transverse to fibres were examined, together with equivalent longitudinal sections. These were then etched similarly to the previous work [3], except that for both transverse and longitudinal sections a reagent with added water was used to reveal the salient detail. This consisted of 1% wt/vol potassium permanganate dissolved in a mixture of 10 vol concentrated sulfuric acid, 4 vol orthophosphoric acid (minimum 85% reagent from Merck) and 1 vol distilled water. Specimens were shaken in this reagent at room temperature for 2 h and then recovered in the usual way. The etched surfaces were replicated in two stages, a first-stage cellulose acetate cast being shadowed with tantalum/tungsten and coated with carbon to give the final replica from which the cellulose acetate was removed by solvent extraction. Replicas were examined in the transmission electron microscope.

2.4. Mechanical measurements

The process of hot compaction of unidirectionally arranged fibres as observed for PE involves a compromise in mechanical properties between the longitudinal modulus, which falls as the compaction temperature is increased and more of the original fibre is melted, and the transverse strength, which rises under the same conditions. The reason for the increase in the transverse strength is because, as described above, once the fibres are compacted together, the weakest part of the structure is within the fibres themselves and this weakness is reduced as the internal structure of the fibres is progressively melted and recrystallized.

The important properties to measure were therefore the longitudinal modulus and transverse strength of the compacted PP samples. Strips, 5 mm wide, were cut from the compacted sheets and tested in three-point bending (ASTM D790) on an Instron tensile testing machine.

3. Results and discussion

3.1. Mechanical properties

Fig. 1 shows values of longitudinal modulus and transverse strength for samples of unidirectional PP compacted over the temperature range 164–174 °C. As can be seen from the results, the transverse strength of

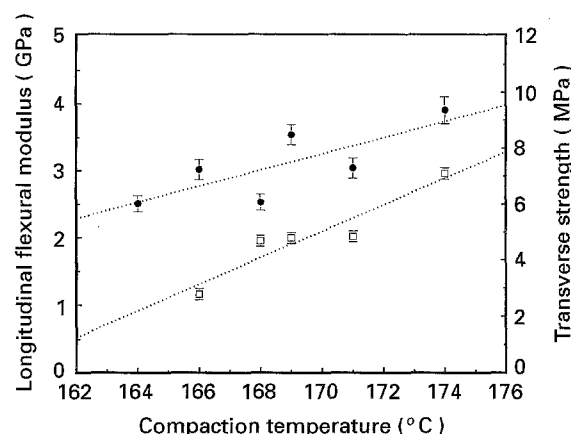


Figure 1 (●) Longitudinal flexural modulus and (□) transverse flexural strength for samples of polypropylene compacted over a range of temperatures.

all the samples is very low, only reaching 7 MPa at the highest compaction temperature so far achieved of 174 °C. This compares with values of around 25 MPa for compacted melt-spun PE and PET samples. The longitudinal modulus values are also on the low side, reaching 3.9 GPa at 174 °C, which is a 55% retention of the original fibre modulus; this compares to a 90% retention for the melt-spun PE and PET fibres previously studied.

An interesting aspect of these results is that both the longitudinal modulus and transverse strength continue to rise as the compaction temperature is increased up to the maximum achievable temperature of 174 °C. This contrasts with the work on the melt-spun PE and PET fibres reported previously, where a balance was found between increasing transverse strength and falling longitudinal modulus as the compaction temperature approached the maximum achievable temperature. The results shown in Fig. 1 appear to indicate that even at the maximum achievable compaction temperature, controlled selective melting, in a significant percentage, is not being achieved.

3.2. Differential scanning calorimetry

In order to assess the value of DSC analysis for determining the compaction mechanisms for a particular fibre, it is useful to perform the following experiment on the uncompact fibre. Fibres are held with constraint in a DSC pan, melted by scanning at 10 K min⁻¹ from 110–190 °C, cooled at (nominally) 200 K min⁻¹ and then remelted as before at 10 K min⁻¹. Fig. 2 shows the results of this experiment on the PP fibre used in this work. It is seen that after complete melting and recrystallization, the rescanned sample shows a similar melting peak to the original: the peak is quite broad in both cases. This result indicates that DSC does not discriminate well between the original fibre and any melted and reformed material produced during a compaction experiment, because the two peaks substantially overlap.

It is interesting to note that the highest possible compaction temperature employed, 174 °C, is well

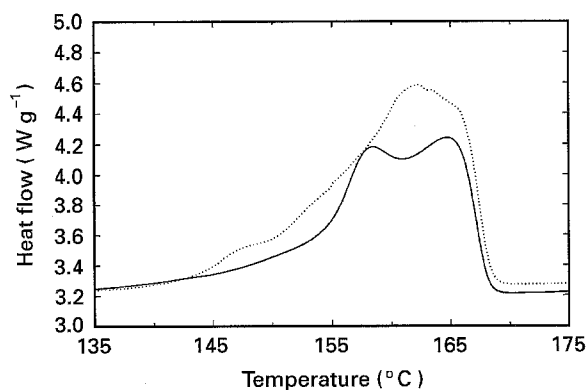


Figure 2 DSC endotherms for (—) the uncompacted fibre and (---) after melting and rescanning.

after the end of the melting endotherm of the original fibre, and this aspect is currently under further investigation.

3.3. Morphological analysis

The observations reported are on two samples compacted at the current highest practicable temperatures, 173 and 174 °C, which we would expect to show the highest fraction of melted and reformed material. Transverse and longitudinal sections have been examined after permanganic etching and reveal morphologies which have been interpreted in part by comparison with previous extensive examinations of compacted melt-spun polyethylene fibres. The results show that despite the high temperatures employed the nature of the compaction is similar to that achieved at sub-optimal temperatures in polyethylene. It is therefore concluded that the relatively poor mechanical performance of the compacted composites is due to a low percentage of "selective" melting of the fibre surfaces.

Fig. 3a is of an etched transverse section following compaction at 173 °C. It shows a hexagonal network of boundaries between fibres with prominent white shadows at the nodes of the mesh. As the electron microscope specimen is itself a two-stage replica, which was shadowed at the first stage, the shadows identify deep holes into the compaction at the network junctions. In fact, the residual replicating material which penetrated the holes and gives the shadows is identifiable as single black lines emanating from each node [3]. This is a situation which is somewhat analogous to melt-spun polyethylene fibres following compaction at 134 °C, in its tendency for originally circular cross-sections to become polygonal, and was due to the compaction temperature of 134 °C being too low to melt a significant percentage of the surface of the fibres. It was seen for the polyethylene samples that when a sufficient fraction of the fibre surface was melted, that this molten layer cushioned the fibres during the high-pressure compaction stage, with the result that the fibres in the compacted composite remained circular in shape. Here, however, the boundaries are essentially planar and the interstices (Fig. 3b) are tiny but deep, again suggesting a lack of a substantial molten phase.

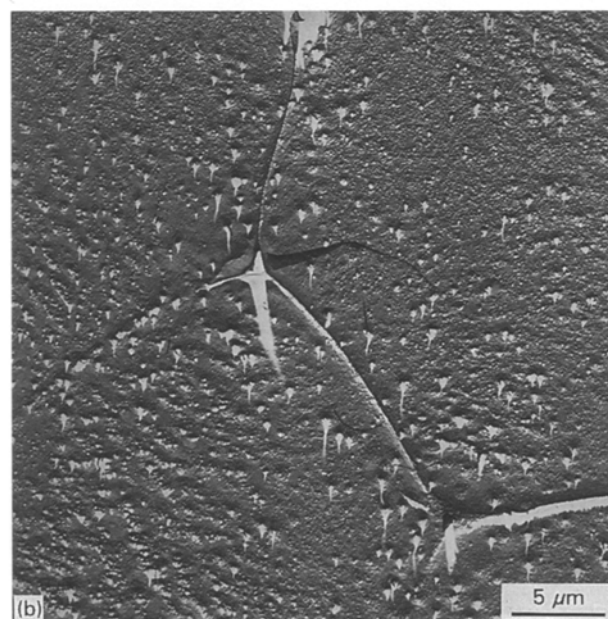
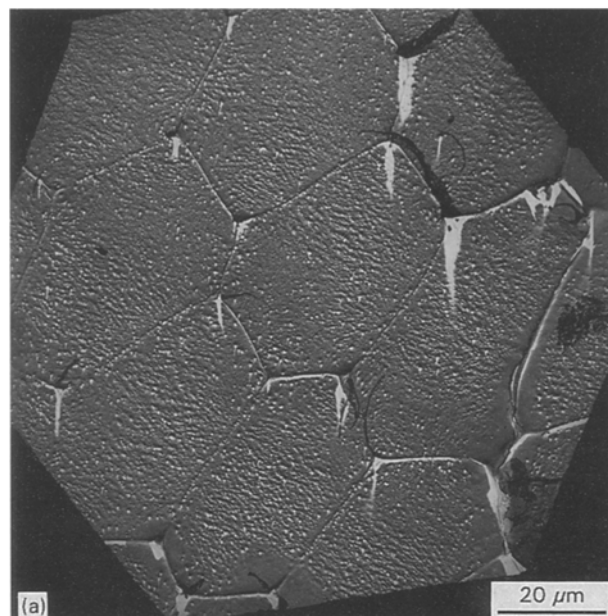


Figure 3 Compaction at 173 °C: etched transverse section showing (a) general structure, and (b) detail of boundaries between fibres.

It is noteworthy in Fig. 3 that there is difference in character between different components of the boundary mesh. Whereas the shorter members are continuous grooves in Fig. 3a, the long sides have a spotty appearance and consists of a series of separate craters. At the higher magnification of Fig. 3b the difference is shown in detail with the boundary to the left of centre being discontinuous as opposed to the continuous central boundary. This distinction is likely to reflect the anisotropic applied stress which has given irregular hexagons. The discontinuous boundaries are those which are normal to the compressive stress and indicate a greater degree of fusion of compacted fibres across their interface. There is much detail within the fibres of a kind that has not been observed in polyethylene. As will become evident for compactations at 174 °C, it is associated, at least in part, with shear

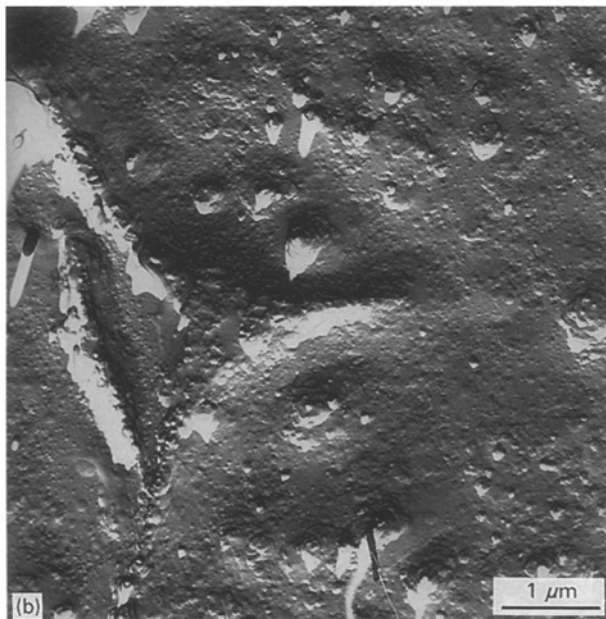
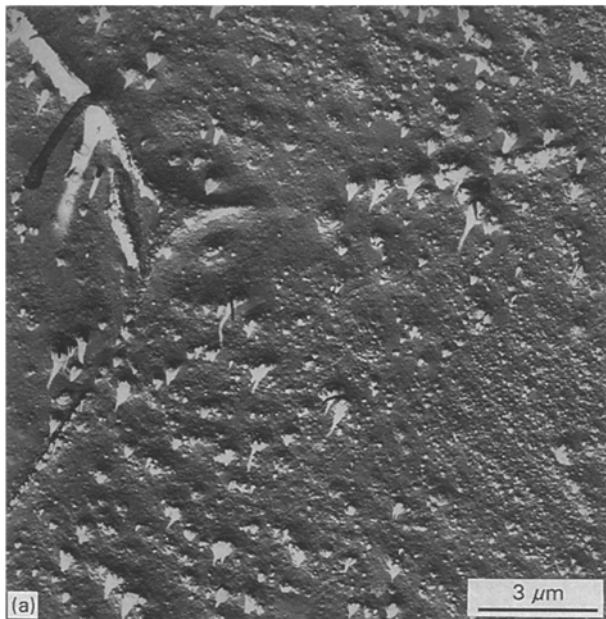


Figure 4 Compaction at 173 °C: detail of Fig. 3 showing (a) a triangular interstice, and (b) detail of material filling the interstice.

deformation which has transformed the shape of the cross-section at constant volume. Note also the different depths of the small craters giving this detail within the compacted fibres; these are identifiable from the shadow lengths in Fig. 3b.

The contrasting nature of the different boundaries is brought out further in Fig. 4a which illustrates three boundaries meeting at a “triangular” interstice. The interface linking the upper left corner is effectively continuous while that to the right of the node is very discontinuous with only a few etched craters interrupting areas where the contacting fibres have fused. The third boundary, extending downwards and to the left, has a character intermediate between the two just described. The interstice itself is filled with lamellar material (Fig. 4b) but the individual lamellae are narrow, as is normal for polypropylene, and much less broad than is the case for polyethylene in similar geometries between compacted fibres.

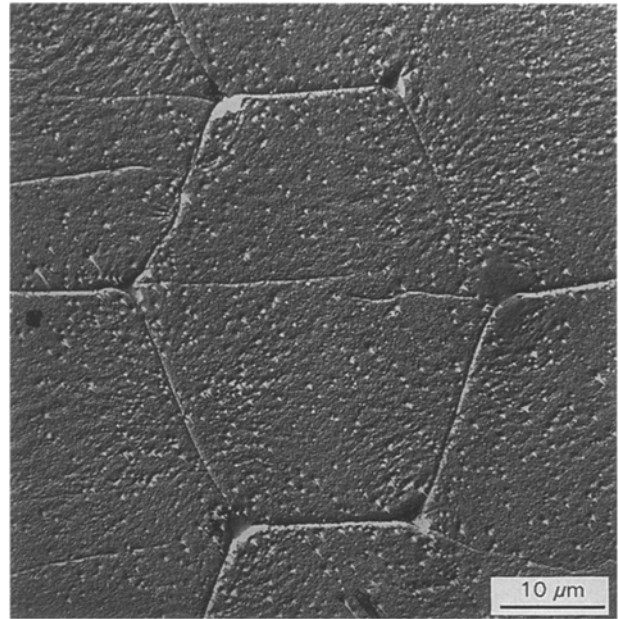


Figure 5 Compaction at 173 °C: etched transverse section through a region showing boundaries in addition to those between fibres.

The area shown in Fig. 5 is atypical in that its hexagonal boundaries are supplemented by others mostly linked to a node of the network and lying horizontal in the figure. These are additional etched grooves which lie within the compacted fibres rather than defining their boundaries. It may be that, lying perpendicular to the longest direction of the hexagon, i.e. to a tensile stress, they represent a vestigial precursor of tensile failure. Incomplete fusion of the neighbouring fibrous interfaces on one side of a node would concentrate the tensile stress in just these regions within the fibre on the opposite side of the junction.

Longitudinal sections provide complementary evidence of patchy fusion, due to an insufficient molten phase. Running diagonally across Fig. 6a is an interfibrillar boundary which appears spotty especially at the bottom of the photograph. Towards the top, from which the detail of Fig. 6b is taken, there is more complete fusion but the boundary is still a shallow groove; the implication is that there has been greater penetration of etchant in this region, in the higher levels that have been removed. This is likely to be a further consequence of sporadic fusion between adjacent fibres. Internally, the fibre occupying the upper left of Fig. 6a displays longitudinal defects some micrometres long parallel to its axis which have also been etched more deeply.

The change in character for compaction at 174 °C can be seen in the transverse section in Fig. 7a. Note especially the fact that the interfibrillar boundaries have, in some instances, disappeared, indicating that the fibres on either side have fused fully. The detail in Fig. 7b illustrates such “absent” boundaries which would have been linked to the node with the longest shadow towards the top of Fig. 7b and at the centre of Fig. 7a. In the middle of Fig. 7b are many bands inclined at approximately 60° to each other and formed from a series of craters. These are presumably

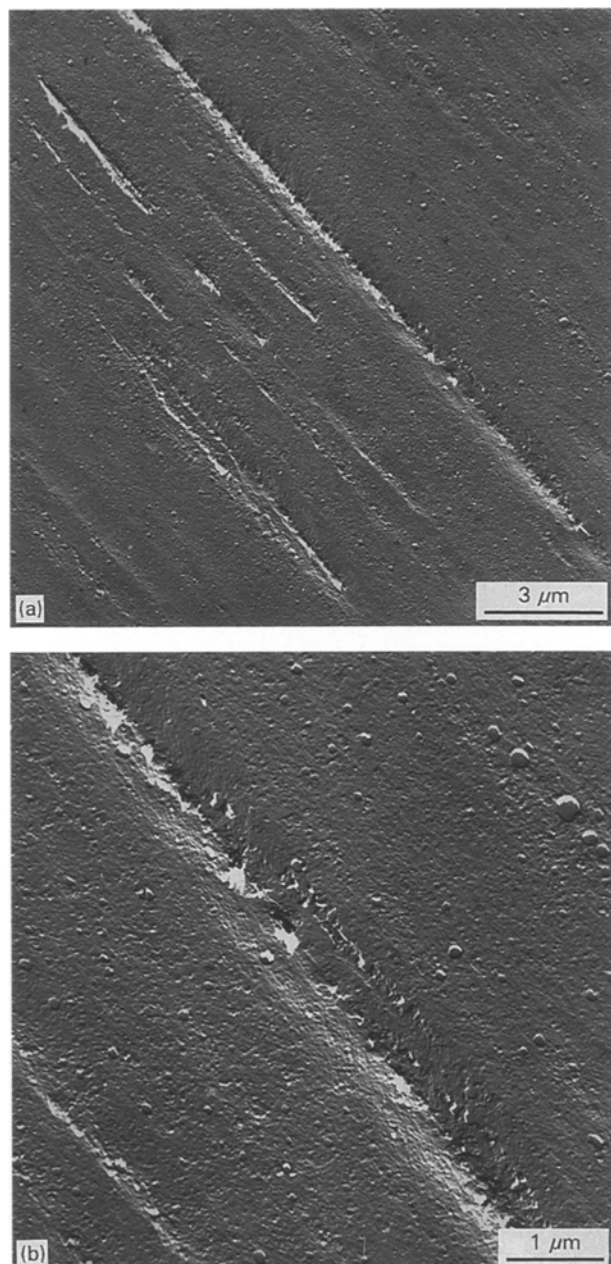


Figure 6 Compaction at 173 °C: (a) etched longitudinal section through a region showing interfibrillar boundaries; (b) detail from (a) in a part showing more complete fusion.

shear bands and a legacy of substantial deformation in a region in which no interfibrillar boundary is now demarcated. Two types of node may be identified. Those in the majority in Fig. 7a are associated with a long shadow, i.e. a deep groove, as for the lower compaction temperature. However, others, which are clearly filled with lamellae, have no such shadow. One is illustrated in Fig. 7c and d which show detail of a node at 1 o'clock from the centre of Fig. 7a. The associated shadow length is less than that of those adjacent within the three neighbouring fibres and is consistent with limited penetration of a texture of lamellae of limited width.

Fig. 8a shows a longitudinal section of a 174 °C compaction containing two different kinds of boundary. The one linked to the lower right-hand corner is a common type. The band to the left, whose detail is

shown in Fig. 8b, is a much rarer phenomenon and shows details of recrystallized lamellae in contrast to the former which is simply a featureless groove.

There are three areas to the centre of Fig. 8b, in addition to the grooves to the left, indicating defective regions within that fibre. At either side of the band and more so on the right than the left, lamellae are seen to enter the band, nucleated on their respective fibres. They are normal to the page and to the fibre axis, with which they share a common chain axis. Especially on the right-hand side there is a change of depth, presumably associated with the etchant following the contour of the underlying fibre. Intervening cross-hatched lamellae are just evident as fine lines approximately parallel to the fibre axis.

The projected widths of these recrystallized lamellar regions, nearly 4 µm on the right and 1 µm on the left, when compared with the previous views, e.g. of Fig. 3b, are too large to be contained within one interstice. Most likely the right-hand side does represent lamellae within a node, with the left-hand side represented on a nearby interfibrillar boundary.

The left centre of the band would, therefore, represent original material which has not melted and recrystallized. There is support for this view in the internal defects clearly visible in the longitudinal extension of this band in Fig. 8a. Nevertheless, the texture in the left centre of the band of Fig. 8b is more organized than that of either fibrous interior to right or left. It has the appearance of a cross-hatched texture growing normal to the page which is the lamellar orientation of the underlying fibre. Probably, therefore, it reveals a sharpening of this texture achieved by annealing, i.e. melting plus recrystallization on a sub-lamellar scale.

The sum of all the above evidence is that under the compaction conditions employed, fibres have not fused to an optimum degree – higher temperatures were difficult to use due to a combination of the increased force of retraction and the fibres being too soft to process. The rather precise hexagonal boundaries of Fig. 3 are evidence of equally soft fibres being substantially deformed without significant fusion, conditions which, as in the polyethylene work, are presumably associated with the earliest stages of melting. The variable extent of fusion is affected to some extent by the applied pressure as shown by the differential contrast of boundaries in Fig. 1b. When boundaries disappear completely, as in Fig. 7b, then this is linked with considerable intrafibrillar cratering and shear deformation. It does not seem that the fusion which is effected is just a simple connection at the boundaries, but at these temperatures is part of a wider change involving a larger body of the two fibres.

It is also noteworthy that, in contrast to successfully compacted melt-spun polyethylene fibres, the intrafibrillar defects have not so far initiated local melting, itself a further indication that the temperatures chosen are at the beginning of melting. Once again the defective regions are deficient in density. Other parallel studies have shown that these develop with increasing extension in the drawing process [6], whereas in polyethylene they were linked to the manner of crystallization.

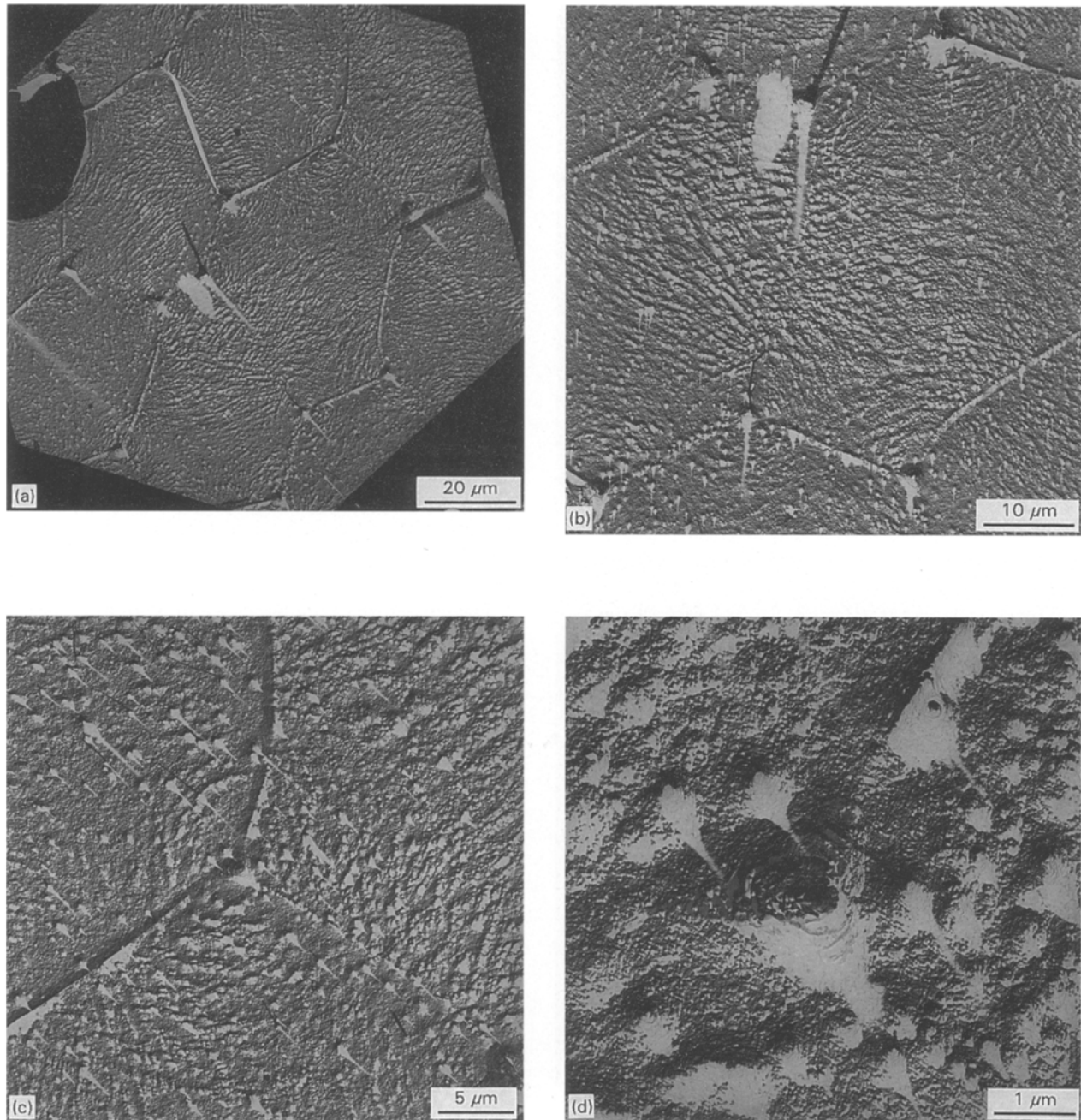


Figure 7 Compaction at 174 °C: etched transverse section showing (a) general structure, (b) detail of an “absent” boundary, (c) a triangular interstice, and (d) detail of material filling the interstice.

The crucial aspect in terms of mechanical properties is whether, under different conditions of temperature, time and pressure to those used here, substantial “selective” melting of the fibre surfaces could be achieved. If a lower holding pressure is used to aid fibre melting, large-scale shrinkage occurs and orientation, and hence fibre modulus, is lost. A window may exist where these properties could be “traded off”, and this is currently under investigation. An alternative route to “trading off” modulus and strength is to use woven polypropylene cloth as the starting material, rather than unidirectionally arranged fibres as described here. As an example, woven polypropylene cloth, compacted at 174 °C, has been measured to have a modulus of 2 GPa and a strength of 30 MPa. This is

also the focus of further study and will be reported in due course.

4. Conclusion

The results presented in this paper show that for the particular high-tenacity polypropylene fibre studied here, at the maximum attainable compaction temperature, “selective” surface melting of the fibre surfaces is not achieved to a sufficient degree to give good mechanical properties. Morphological analysis shows features which are similar in broad detail to samples of melt-spun polyethylene compacted at 134 °C, which is considered sub-optimal. The lack of controlled melting could be a consequence of the high shrinkage

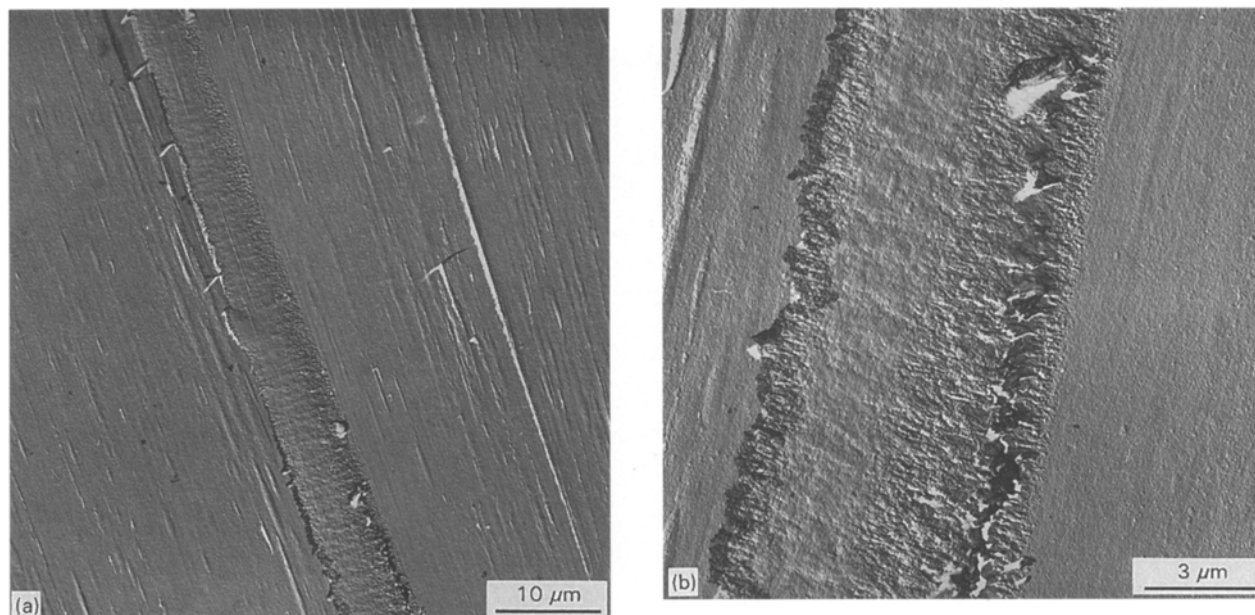


Figure 8 Compaction at 174 °C: (a) etched longitudinal section through a region showing two types of interfibrillar boundaries, and (b) detail from (a) showing lamellar growth at a boundary.

forces seen with this fibre, resulting in the need to use a high holding pressure during heating to stop the fibres shrinking.

Acknowledgement

The authors thank F. Drake and Co. Ltd for supplying the polypropylene fibre.

References

1. P. J. HINE, I. M. WARD, R. H. OLLEY and D. C. BASSETT, *J. Mater. Sci.* **28** (1993) 316.
2. J. RASBURN, P. J. HINE, I. M. WARD, R. H. OLLEY, D. C. BASSETT and M. A. KABEEL, *ibid.* **30** (1995) 615.
3. R. H. OLLEY, D. C. BASSETT, P. J. HINE and I. M. WARD, *ibid.* **28** (1993) 1107.
4. M. A. KABEEL, R. H. OLLEY, D. C. BASSETT, P. J. HINE and I. M. WARD, *ibid.* **29** (1994) 4694.
5. *Idem*, *ibid.* **30** (1995) 601.
6. M. I. ABO EL MAATY, D. C. BASSETT, R. H. OLLEY, M. G. DOBB, J. G. TOMKA and I.-C. WANG, *Polymer*, accepted.

Received 8 August
and accepted 8 September 1995